

Large Seebeck coefficient resulting from chiral interactions in triangular triple quantum dots

Yi-Ming Liu(刘一铭) and Jian-Hua Wei(魏建华)

Citation: Chin. Phys. B, 2022, 31 (**9**): 097201. DOI: 10.1088/1674-1056/ac6dae
Journal homepage: http://cpb.iphy.ac.cn; http://iopscience.iop.org/cpb

What follows is a list of articles you may be interested in

Capacitive coupling induced Kondo-Fano interference in side-coupled double quantum dots

Fu-Li Sun(孙复莉), Yuan-Dong Wang(王援东), Jian-Hua Wei(魏建华), Yi-Jing Yan(严以京)
Chin. Phys. B, 2020, 29 (**6**): 067204. DOI: 10.1088/1674-1056/ab8ac1

Electrically tunable spin diode effect in a tunneling junction of quantum dot

Xukai Peng(彭许凯), Zhengzhong Zhang(张正中)
Chin. Phys. B, 2019, 28 (**12**): 127202. DOI: 10.1088/1674-1056/ab53d0

Magnetotransport properties of graphene layers decorated with colloid quantum dots

Ri-Jia Zhu(朱日佳), Yu-Qing Huang(黄雨青), Jia-Yu Li(李佳玉), Ning Kang(康宁), Hong-Qi Xu(徐洪起)
Chin. Phys. B, 2019, 28 (**6**): 067201. DOI: 10.1088/1674-1056/28/6/067201

Direct spin-phonon coupling of spin-flip relaxation in quantum dots

Ji-Wen Yin(尹辑文), Wei-Ping Li(李伟萍), Hong-Juan Li(李红娟), Yi-Fu Yu(于毅夫)
Chin. Phys. B, 2017, 26 (**1**): 017201. DOI: 10.1088/1674-1056/26/1/017201

Decrease of back recombination rate in CdS quantum dots sensitized solar cells using reduced graphene oxide

Ali Badawi
Chin. Phys. B, 2015, 24 (**4**): 047205. DOI: 10.1088/1674-1056/24/4/047205

Large Seebeck coefficient resulting from chiral interactions in triangular triple quantum dots

Yi-Ming Liu(刘一铭) and Jian-Hua Wei(魏建华)†

Department of Physics, Renmin University of China, Beijing 100872, *China*

(Received 4 March 2022; revised manuscript received 22 April 2022; accepted manuscript online 7 May 2022)

We theoretically study thermoelectric transport properties through a triangular triple-quantum-dot (TTQD) structure in the linear response regime using the hierarchical equations of motion approach. It is demonstrated that large Seebeck coefficient can be obtained when properly matching the interdot tunneling strength and magnetic flux at the electron–hole symmetry point, as a result of spin chiral interactions in the TTQD system. We present a systematic investigation of the thermopower (the Seebeck coefficient) dependence on the tunneling strength, magnetic flux, and on-site energy. The Seebeck coefficient shows a clear breakdown of electron–hole symmetry in the vicinity of the Kondo regime, accompanied by the deviation from the semiclassical Mott relation in the Kondo and mixed-valence regimes, which result from the many-body effects of the Kondo correlated induced resonance together with spin chiral interactions.

Keywords: quantum dots, Seebeck coefficient, thermoelectric transport

PACS: 73.21.La, 72.15.Jf **DOI:** 10.1088/1674-1056/ac6dae

1. Introduction

Recently, the field of thermoelectricity has fed an intense interest in nanostructure devices because of its potential applications in highly efficient thermoelectric devices. The violation of the Wiedemann–Franz law[1,2] in these devices makes it possible to achieve much higher thermoelectric efficiency.[3–7] The thermoelectric efficiency of a material is measured by the dimensionless thermoelectrical figure of merit $ZT = S^2\sigma T/\kappa$, where S is the Seebeck coefficient, σ is conductance, and κ is thermal conductivity. Recent studies indicate that zero-dimensional quantum dot structures result in novel thermoelectric phenomena and significantly increase thermoelectric efficiency.[8–10]

In these studies, the Seebeck coefficient (thermopower) is an important parameter characterizing the thermoelectric transport properties of quantum dot (QD) systems, which plays a significant role in improving thermoelectric efficiency. In general, the magnitude and sign of the thermopower can be changed by tuning the gate voltage,[11] level shift space,[12] and interdot tunneling[13] through the QDs. For a QD embedded in a ring structure, the Aharonov–Bohm-type oscillations of the Seebeck coefficient have indicated that the thermopower strongly depends on the flux.[14] Consequently, the thermopower can be used as an experimental tool to study the phase-sensitive Aharonov–Bohm interferometer.[15] Moreover, the thermopower is a direct measurement of the weighted spectral density of the states in correlated systems with respect to the Fermi energy. Therefore, we can easily obtain information concerning electron-like or hole-like transport by calculating the Seebeck coefficient of a QD system. In experiments, the Seebeck coefficient is primarily derived via current heating[16] and electron heating techniques.[11,17] Some experimental studies have shown a clear breakdown of transport electron–hole symmetry in the vicinity of Kondo spin correlations, accompanied by deviations from the semiclassical Mott relation,[11,18,19]

$$S_{\rm Mott} = -\frac{\pi^2}{3}\frac{k_{\rm B}^2 T}{e}\frac{\partial \ln G(\varepsilon)}{\partial \varepsilon}, \tag{1}$$

which describes the relationship between the thermopower S and conductance G, with $k_{\rm B}$ being Boltzmann constant and ε the gate voltage. Theoretical researches have focused on strongly correlated QDs, and the Seebeck coefficient has been shown to be a very sensitive and powerful tool to study the Kondo effect. The Seebeck coefficient manifests itself as an energy peak in the density of state slightly above the Fermi energy, leading to a change in the sign of the thermopower. For example, the Seebeck coefficient exhibits two sign changes in the Kondo regime, showing that the thermopower is sensitive to the Kondo resonance scattering of conduction electrons[20] and that the thermocurrent charge polarity reverses with a significantly enhanced magnitude at low temperatures as a result of the formation of a Kondo singlet.[21]

In addition, triple quantum dots (TQD) with various structures have been theoretically studied and prepared in experiments, exhibiting rich many-particle interactions. Such studies have focused on the stability diagram, electron transport, quantum interference effect, and thermoelectric transport.[13,22–29] In particular, the thermoelectric transport properties in serially TQD structure have already been investigated,[13] showing that the Seebeck coefficient is strongly enhanced near the subradiant state, leading to the enhancement of the thermoelectric efficiency. Moreover, the

†Corresponding author. E-mail: wjh@ruc.edu.cn

© 2022 Chinese Physical Society and IOP Publishing Ltd

triangular triple-quantum-dot (TTQD) system has additional extended freedoms and complex geometrical configurations, which are expected to enable various many-body effects in the strongly correlated regime,[26,27] and has interesting thermoelectric transport properties because of the existence of the quantum interference effect.[28,29] In addition, the spin chirality induced by the noncoplanar spin configuration[30] in the TTQD structure exhibits rich physical phenomena, such as the application of spin chiral interactions in quantum computation via spin cluster qubits,[30,31] as well as a bias-induced chiral current resulting from the splitting of the degeneracy of the chiral states in TTQD system.[33] However, to the best of our knowledge, thermoelectric transport through the TTQD system remains less studied, particularly transport accounting for the influence of spin chiral interactions.

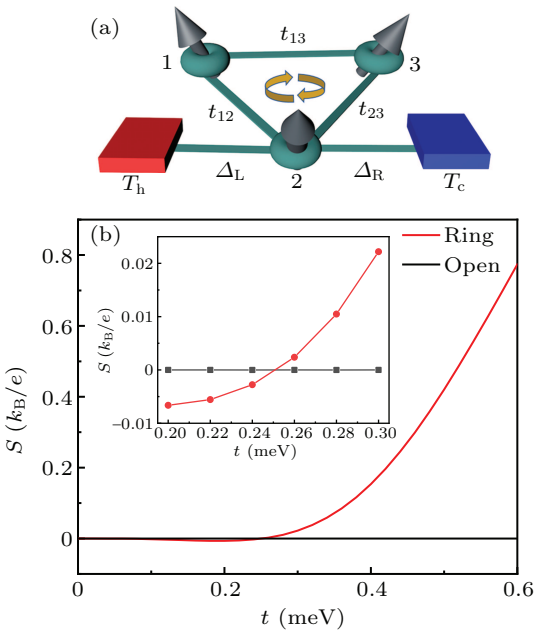


Fig. 1. (a) Schematic of thermoelectric transport through the TTQD system. The QD2 is tunneling coupled to two reservoirs via the dot-lead coupling strength $\Delta_{L/R}$, $\Delta = 2\Delta_{L/R} = 0.5$ meV in this paper, three quantum dots are coupled with each other through tunneling strength t. The left reservoir (red) is the hot bath and the right reservoir (blue) is the cold bath. The temperature gradient is $\Delta T = T_h - T_c$, $k_B\Delta T = 0.002$ meV in this work. (b) The Seebeck coefficient S as a function of interdot tunneling strength t at the electron–hole symmetry point without magnetic field. The ring structure (red solid line) is calculated in the TTQD structure with the same interdot tunneling strength $t_{12} = t_{13} = t_{23}$; the open structure (black solid line) is calculated in serially coupled TQD structure, namely the tunneling strength t_{13} between QD1 and QD3 is zero. The other parameters for the system are taken as $U = 2$ meV, $\varepsilon = -1$ meV, the bandwidth is $W = 0.5$ meV and the temperature for system is $k_BT = 0.2$ meV.

On the basis of the above research results and applications, we propose a system composed of three triangularly configured and coupled QDs, with one dot (QD2) connected to two electron reservoirs via the dot-reservoir coupling strength $\Delta_{L/R}$, as schematically shown in Fig. 1(a). The temperature of the system is defined as $T = (T_h - T_c)/2$. The electron on each dot is single occupation, i.e., spin $= 1/2$, and moves through the three QDs in the clockwise or anticlockwise direction. Three noncoplanar spin structures contribute to the spin chiral operator $S_1 \cdot (S_2 \times S_3)$ of the chiral interaction in the TTQD system. The chiral interactions involving both spin and orbital degrees of freedom generated in the TTQD system lead to novel thermoelectric transport behavior, which differs vastly from the thermoelectric properties in the serially TQD structure. As shown in Fig. 1(b), a large Seebeck coefficient for the ring structure (solid red line) of the TTQD system is obtained with the increasing interdot tunneling strength t, $(t_{12} = t_{13} = t_{23})$. Conversely, S remains at a value of zero for a open structure (solid black line) of the serially TQD, where the interdot tunneling between QD1 and QD3 is zero and $t_{12} = t_{23} = t$.

In this paper, we analyze the thermoelectric effects in a tunneling-coupled TTQD system coupling two metal leads. The basic thermoelectric coefficients in the linear response regime are obtained using the hierarchical-equations-of-motion (HEOM) approach. We present a systematic investigation of the influence of the tunneling strength t, the magnetic flux ϕ, and the on-site energy ε, on the Seebeck coefficient S (thermopower), through the TTQD system. We demonstrate that a large Seebeck coefficient can be obtained when properly matching the interdot tunneling strength via a ring-like TTQD system, as a result of the formation of spin chiral interactions; whereas S for the serially TQD remains at zero. Numerical computation results show that the semiclassical Mott relation between the thermopower and conductance is failed to describe the asymmetry of the electron–hole transport in the Kondo and mixed-valence regimes. This is attributed to the many-particle nature of the Kondo correlation induced resonance together with the spin chiral interactions through the TTQD system.

2. Theory and approach

2.1. Model and Hamiltonian

We adopt Anderson imparity model to represent the TTQD system in this work. The total Hamiltonian is

$$H_{\rm tot} = H_{\rm dots} + H_{\rm res} + H_{\rm coup}. \tag{2}$$

The dots is described as

$$H_{\rm dots} = \sum_{i\mu} \varepsilon_i \hat{d}^\dagger_{i\mu}\hat{d}_{i\mu} + U\sum_i \hat{n}_{i\uparrow}\hat{n}_{i\downarrow} + \sum_{i\neq j\mu} t_{ij}\hat{d}^\dagger_{i\mu}\hat{d}_{j\mu}, \tag{3}$$

where $d^\dagger_{i\mu}$ $(d_{i\mu})$ creates (annihilates) an electron of spin μ on the i-th dot with single-electron energy level ε_i, and $n_{i\mu} = d^\dagger_{i\mu}d_{i\mu}$ is the operator of the occupation number on the i-th dot. The t_{ij} term is the tunneling coupling between two QDs and is determined by the overlap integral of their wave functions.

The noninteracting electron reservoir in the two leads are described by $H_{\rm res} = \sum_{\alpha k\mu} \varepsilon_{\alpha k} c^\dagger_{\alpha k\mu} c_{\alpha k\mu}$, where $c^\dagger_{\alpha k\mu}$ $(c_{\alpha k\mu})$ creates (annihilates) an electron on the k-th state of lead α.

The interactions between QDs and the leads are $H_{\rm coup} = \sum_{\alpha k i\mu} V_{\alpha k i\mu} d^{\dagger}_{i\mu} c_{\alpha k\mu} + {\rm H.c.}$ with $V_{\alpha k i\mu}$ being the tunnel matrix element between i-th impurity and electrons with k-th state on the α-reservoir. When we focus on QD2 in this paper, $V_{\alpha k\mu}$ is the electron tunneling strength between two leads and QD2. The effect of electron reservoirs on QDs is taken into account through the hybridization functions, $\Delta_{\mu\nu}(\omega) \equiv \Sigma_\alpha \Delta_{\alpha\mu\nu}(\omega) = \pi \Sigma_{\alpha k} V_{\alpha\mu k} V^{*}_{\alpha\nu k} \delta(\omega - \varepsilon_{\alpha k})$, in the absence of applied chemical potentials. Generally, we adopt Lorentzian hybridization functions in the HEOM approach, that is, $\Delta_{\mu\nu}(\omega) = \delta_{\mu\nu} \Delta W^2/(\omega^2 + W^2)$, with $\Delta = \Sigma_\alpha \Delta_\alpha$ being the overall dot-lead coupling strength and W the bandwidth of the electrodes.

Thermopower (TP) is usually characterized by the Seebeck coefficient, which is defined as[7,18]

$$S_{\rm def} \equiv -\left(\frac{V_{\rm T}}{\Delta T}\right)_{I=0} = \left(\frac{V}{\Delta T}\right)_{I=0}. \tag{4}$$

We can measure the Seebeck coefficient by searching for the bias voltage V that cancels $V_{\rm T}$,[7] with the HEOM approach, $S_{\rm def}$ can be computed precisely by following the definition of Eq. (3).[12] While it is computationally more convenient to focus on the linear regime, the total current is[3]

$$I = GV + L_{\rm T} \Delta T, \tag{5}$$

hence, the thermopower (TP) can be evaluated as

$$S_{\rm linear} = -\frac{L_{\rm T}}{G}, \tag{6}$$

where the coefficient $L_{\rm T} = (\frac{\partial I}{\partial \Delta T})_{V=0}$ and the conductance $G = (\frac{\partial I}{\partial V})_{\Delta T=0}$ can be obtained by computing the thermocurrent or electronic current response to a small temperature gradient ΔT and a small bias voltage V, respectively.

Under a perpendicular magnetic field, the magnetic flux ϕ threads the ring-like TTQD structure, we assume the magnetic flux act on the interdot tunneling t, that is, $\widetilde{t} = {\rm e}^{\pm {\rm i}\frac{2\pi}{3}\phi/\phi_0} t$. Then the t–J–χ effective model can be derived by treating t in $H_{\rm dots}$ perturbatively, up to the third order[33,34]

$$\begin{aligned} H_{\rm eff} \;=\; & -t(1-n) \sum_{ij,\mu} (\widehat{d}^{\dagger}_{i\mu} \widehat{d}_{j\mu} + {\rm H.c.}) \\ & + J \sum_{i<j} \left(\widehat{S}_i \widehat{S}_j - \frac{1}{4} \widehat{n}_i \widehat{n}_j \right) + \chi \widehat{S}_1 \cdot (\widehat{S}_2 \times \widehat{S}_3), \end{aligned} \tag{7}$$

where n is the average occupation number on each dot. The first term will vanish in the half-filling situation ($n = 1$). The second term is Heisenberg exchange interaction with $J = 4t^2/U$. The third term is the chiral term with chiral operator $\widehat{S}_1 \cdot (\widehat{S}_2 \times \widehat{S}_3)$,[35] where χ is the chiral interaction with $\chi = 24 t^3 \sin(2\pi\phi/\phi_0)/U^2$, and ϕ is the magnetic flux enclosed by the TTQD structure. Here, $\phi_0 = hc/e$ is the unit of quantum flux. For simplicity, we let $\varphi = 2\pi\phi/\phi_0$; thus, $\chi = 24 t^3 \sin(\varphi)/U^2$.

2.2. HEOM approach for QDs

The HEOM approach investigates the properties of quantum dots in both equilibrium and non-equilibrium states via the reduced density operator, which has a universal formalism for an arbitrary system Hamiltonian; thus, it can be used to accurately solve the three-impurity Anderson model. We show a brief derivation of the HEOM approach,[36,37] at time t, the reduced system density operator $\rho(t) = {\rm tr}_{\rm res} \rho_{\rm T}(t)$ is related to the initial value at time t_0 via the reduced Liouville-space propagator $\mathcal{G}(t, t_0)$ by

$$\rho(t) = \mathcal{G}(t, t_0) \rho(t_0). \tag{8}$$

Let $|\psi\rangle$ be an arbitrary basis set defined in system space, and $\psi = (\psi, \psi')$. Therefore, $\rho(\psi, t) = \rho(\psi, \psi', t)$. From the Feynman–Vernon influence functional, the path-integral expression for the reduced Liouville-space propagator is

$$\mathcal{G}(\psi, t; \psi_0, t_0) = \int_{\psi_0[t_0]}^{\psi[t]} \mathcal{D}\psi \, {\rm e}^{{\rm i}S[\psi]} \mathcal{F}[\psi] \, {\rm e}^{-{\rm i}S[\psi']}. \tag{9}$$

Here, $S[\psi]$ is the classical action of the reduced system, $\mathcal{F}[\psi]$ is the influence functional determined by the Grassmann variables of the system-environment coupling $f^{\dagger}_{\alpha i\mu}(t) d_{i\mu}[\psi_\mu] + {\rm H.c.}$ The operators $f^{\dagger}_{\alpha i\mu}(t)$ and $f_{\alpha i\mu}(t)$ are the reservoir operators defined by

$$f^{\dagger}_{\alpha i\mu}(t) \equiv {\rm e}^{{\rm i}H_\alpha t} \left(\sum_{k\in\alpha} V^{*}_{\alpha k i\mu} c^{\dagger}_{\alpha k\mu} \right) {\rm e}^{-{\rm i}H_\alpha t}, \tag{10}$$

$$f_{\alpha i\mu}(t) \equiv {\rm e}^{{\rm i}H_\alpha t} \left(\sum_{k\in\alpha} V_{\alpha k i\mu} c_{\alpha k\mu} \right) {\rm e}^{-{\rm i}H_\alpha t}. \tag{11}$$

The influence functional can be evaluated using the Wick theorem and the second-order cumulant expansion method, because all the other higher order cumulants are zero at the thermodynamic Gaussian average for non-interaction leads. As a result, the ensemble average of the second-order cumulants is connected to the reservoir correlation functions $C^{\pm}_{\alpha ij\mu}(t)$, defined as

$$C^{+}_{\alpha ij\mu}(t) = \left\langle f^{\dagger}_{\alpha i\mu}(t) f_{\alpha j\mu}(0) \right\rangle_{\rm res}, \tag{12}$$

$$C^{-}_{\alpha ij\mu}(t) = \left\langle f_{\alpha i\mu}(t) f^{\dagger}_{\alpha j\mu}(0) \right\rangle_{\rm res}, \tag{13}$$

where $\langle \cdots \rangle_{\rm res}$ stands for the ensemble average of the reservoirs, and the time translation invariance is used. All LCFs in a form differ from that in Eqs. (12) and (13), and they are zero because the lead operators $f^{\dagger}_{\alpha i\mu}(t)$ and $f_{\alpha i\mu}(t)$ satisfy Gaussian statistics. The reservoir spectral density function is defined as

$$J_{\alpha ij\mu}(\omega) \equiv \frac{1}{2\pi} \int_{-\infty}^{\infty} {\rm d}t \, {\rm e}^{{\rm i}\omega t} \langle \{ f_{\alpha i\mu}(t), f^{\dagger}_{\alpha j\mu}(0) \} \rangle, \tag{14}$$

with the simplified notation $\sigma = +, -$ and $\bar{\sigma} = -\sigma$, the reservoir correlation functions are associated with the spectral density functions via the fluctuation-dissipation theorem

$$C^{\sigma}_{\alpha ij\mu}(t) = \int_{-\infty}^{\infty} {\rm d}\omega \, {\rm e}^{{\rm i}\sigma\omega t} f^{\sigma}_{\alpha}(\omega) J^{\sigma}_{\alpha ij\mu}(\omega), \tag{15}$$

where $J^{-}_{\alpha ij\mu}(\omega) = J_{\alpha ij\mu}(\omega)$, $J^{+}_{\alpha ij\mu}(\omega) = J_{\alpha ji\mu}(\omega)$, and $f^{\sigma}_{\alpha}(\omega) = 1/(1+\mathrm{e}^{\sigma\beta_\alpha(\omega-\mu_\alpha)})$ is the Fermi–Dirac function for the electron ($\sigma = +$) or hole ($\sigma = -$) at the temperature $\beta_\alpha = 1/k_{\mathrm{B}}T_\alpha$. For linear coupling with a non-interacting reservoir, the reservoir spectral density function can be evaluated as $J_{\alpha ij\mu}(\omega) = \sum_k V^{*}_{\alpha ki\mu}V_{\alpha kj\mu}\delta(\omega-\varepsilon_{\alpha k})$. After applying the Wick theorem and Grassmann algebra, the final expression of the influence functional $\mathcal{F}$ is

$$\mathcal{F}[\psi] = \exp\left\{-\int_{t_0}^{t}\mathrm{d}\tau\mathcal{R}[\tau,\{\psi\}]\right\}, \tag{16}$$

where $\mathcal{R}[\tau,\{\psi\}] = \frac{\mathrm{i}}{\hbar^2}\sum_{\alpha i\mu\sigma}\mathcal{A}^{\bar{\sigma}}_{i\mu}[\psi(t)]\mathcal{B}^{\sigma}_{\alpha i\mu}[t,\psi]$. Here, $\mathcal{A}^{\bar{\sigma}}_{i\mu}$ and $\mathcal{B}^{\sigma}_{\alpha i\mu}$ are the Grassmann variables defined as

$$\mathcal{A}^{\bar{\sigma}}_{i\mu}[\psi(t)] = d^{\sigma}_{is}[\psi(t)] + d^{\sigma}_{is}[\psi'(t)], \tag{17}$$

$$\mathcal{B}^{\sigma}_{\alpha i\mu}[t,\psi] = -\mathrm{i}\left[B^{\sigma}_{\alpha i\mu}(t,\psi) - B'^{\sigma}_{\alpha i\mu}(t,\psi')\right], \tag{18}$$

with

$$B^{\sigma}_{\alpha i\mu}(t,\psi) = \sum_j\int_0^t\mathrm{d}\tau C^{\sigma}_{\alpha ij\mu}(t-\tau)d^{\sigma}_{j\mu}[\psi(\tau)], \tag{19}$$

$$B'^{\sigma}_{\alpha i\mu}(t,\psi') = \sum_j\int_0^t\mathrm{d}\tau C^{\bar{\sigma}*}_{\alpha ij\mu}(t-\tau)d^{\sigma}_{j\mu}[\psi'(\tau)]. \tag{20}$$

The LCFs play the role of memory kernels that can be expanded by a series of exponential functions with implementation of the fluctuation-dissipation theorem together with the Cauchy residue theorem and the Padé spectrum decomposition scheme of the Fermi function

$$C^{\sigma}_{\alpha ij\mu}(t) = \sum_{m=1}^{M}\eta^{\sigma}_{\alpha ij\mu m}\mathrm{e}^{-\gamma^{\sigma}_{\alpha ij\mu m}t}. \tag{21}$$

The influence of bath enters the equations of motion with M exponentiations. The auxiliary density operators (ADOs) $\left\{\rho^{n}_{j} = \rho_{j_1\cdots j_n}\right\}$ are determined by the time derivative of the influence functional. The final form can be reduced to the following compact form:

$$\begin{aligned}\dot{\rho}^{(n)}_{j_1\cdots j_n} =& -\Big(\mathrm{i}\mathcal{L} + \sum_{r=1}^{n}\gamma_{j_r}\Big)\rho^{(n)}_{j_1\cdots j_n} - \mathrm{i}\sum_j\mathcal{A}_{\bar{j}}\rho^{(n+1)}_{j_1\cdots j_n j}\\ &-\mathrm{i}\sum_{r=1}^{n}(-)^{n-r}\mathcal{C}_{j_r}\rho^{(n-1)}_{j_1\cdots j_{r-1}j_{r+1}\cdots j_n},\end{aligned} \tag{22}$$

the index $j \equiv (\sigma\mu m)$ corresponds to the transfer of an electron to/from ($\sigma = +/-$) the impurity state μ, associated with the characteristic memory time γ_m^{-1}, $m_r = 1,\ldots,M$ denotes the poles in the LCF. The Grassmannian superoperators $\mathcal{A}_{\bar{j}} \equiv \mathcal{A}^{\bar{\sigma}}_{i\mu}$ and $\mathcal{C}_j \equiv \mathcal{C}^{\sigma}_{ij\mu m}$ are defined via their fermionic actions on an operator $\hat{O}$ as $\mathcal{A}_j\hat{O} \equiv [\hat{d}^{\bar{\sigma}}_{i\mu},\hat{O}]$ and $\mathcal{C}_j\hat{O} \equiv \eta_j\hat{d}^{\sigma}_{i\mu}\hat{O} + \eta^{*}_j\hat{O}\hat{d}^{\sigma}_{i\mu}$, respectively. The on-dot electron interactions are contained in the Liouvillian of impurities, $\mathcal{L}\cdot \equiv [H_{\mathrm{dot}},\cdot]$. Here, $\rho_0(t) = \rho(t) = \mathrm{tr}_{\mathrm{res}}\rho_{\mathrm{total}}(t)$ is the reduced density matrix and $\{\rho_{j_1,\ldots,j_n}(t)^n; n = 1,\ldots,L\}$ are auxiliary density matrices, with L denoting the truncation level. The transient current through the electrode α is

$$I_\alpha(t) = \mathrm{i}\sum_{i\mu}\mathrm{tr}_{\mathrm{sys}}[\rho^{\dagger}_{\alpha i\mu}(t)\hat{d}_{i\mu} - \hat{d}^{\dagger}_{i\mu}\rho^{-}_{\alpha i\mu}(t)], \tag{23}$$

where $\rho^{\dagger}_{\alpha i\mu} = (\rho^{-}_{\alpha i\mu})^{\dagger}$ is the first-tier auxiliary density operator obtained by solving Eq. (22). The influence of the α-reservoir can be characterized completely by the hybridization function $\Delta_{\mu\nu}(\omega) \equiv \sum_\alpha\Delta_{\alpha\mu\nu}(\omega) \equiv \pi\sum_{\alpha k}V_{\alpha\mu k}V^{*}_{\alpha\nu k}\delta(\omega-\varepsilon_{\alpha k})$. We choose a Lorentzian spectral density function

$$\Delta_{\alpha\mu\nu}(\omega) = \Delta_\alpha\delta_{\mu\nu}\frac{W_\alpha^2}{\omega^2+W_\alpha^2} \tag{24}$$

with a width of the conduction band of W_α on the α lead in the absence of chemical potential. Moreover, the spectral density function for i-th QD with μ-spin can be written as

$$\begin{aligned}&A_{i\mu}(\omega)\\ &= \frac{1}{\pi}\mathrm{Re}\left\{\int_0^\infty\mathrm{d}t\{C_{a_{i\mu}a^{\dagger}_{i\mu}}(t) + [C_{a_{i\mu}a^{\dagger}_{i\mu}}(t)]^{*}\}\mathrm{e}^{-\mathrm{i}\omega t}\right\},\end{aligned} \tag{25}$$

and $A(\omega) = \sum_{i\mu}A_{i\mu}(\omega)$.

The HEOM approach is established based on the Feynman–Vernon influence functional path-integral theory[38] and implemented with Grassmann algebra for fermion dissipations.[39] Basically, the HEOM approach is a nonperturbative method for general quantum systems coupled to reservoir that satisfies Grassmann Gaussian statistics.[39–41] Based on the linear response theory of quantum open systems, we can accurately and efficiently obtain a dynamical observable quantity of strongly correlated quantum impurity systems.[36] In practical calculations, we must minimize the computational expenditure while maintaining the quantitative accuracy. For this purpose, we usually impose a truncation L as the highest tier of the ADOs. This truncation decreases the number of EOMs to match the insufficient calculation capacity, without affecting the nonperturbation characteristic of HEOM. This truncation L is measured by the quantitative convergence at $A(\omega = 0)$ when the Kondo effect is considered, usually $L = 4$ for most physical cases. However, lower temperatures demand a higher truncation tier and more computing resources to achieved numerical convergence. In recent years, the HEOM approach has been widely used to investigate the Kondo effect and transport properties under equilibrium and non-equilibrium conditions in quantum dot systems.[36,42–44]

3. Results and discussions

3.1. Interdot tunneling dependence of thermoelectric transport properties

To distinguish the influence of the tunneling strength t on the Seebeck coefficient S, in the two types of TQD structures, that is, the ring structure for the TTQD system and the open structure for the serially TQD system, we calculate the

Seebeck coefficient for two cases at the electron–hole symmetry point. The on-site energy for each QD is $\varepsilon = -U/2 = -1$ meV, and a diagram is presented in Fig. 1(b). In the TTQD system, the Seebeck coefficient for ring (solid red line) is calculated in a structure where the three QDs coupled with each other via the same tunneling strength t ($t_{12} = t_{13} = t_{23}$). For an open structure (solid black line) calculated in a serially coupled TQD system, the tunneling strength t_{13} between QD1 and QD3 is zero and the S is a function of the tunneling strength t ($t_{12} = t_{23} = t$).

As depicted in Fig. 1(b), the most distinctive feature of the Seebeck coefficient S in the ring structure is a large magnitude with increasing tunneling strength t, compared with the open structure where it maintains a value near zero. In addition, the Seebeck coefficient exhibits different behaviors for weak and strong interdot tunneling strengths. For the ring structure (solid red line) in the TTQD system, the Seebeck coefficient maintains a value of zero for small tunneling strengths, $t \lesssim 0.1$ meV, and the very small coupling strength between QDs causes QD2 to decouple from the other two dots (QD1 and QD3). Therefore, the thermoelectric transport behavior is similar to that of a single QD coupled with two leads, where the thermocurrent maintains a value of zero at the electron–hole symmetry point.[21] That is, the number of electrons transported is equal to the number of holes transported. Hence, the Seebeck coefficient is zero. Meanwhile, with increasing tunneling strength, $t \gtrsim 0.1$ meV, the induced second-order antiferrmomagnetic spin coupling $J = 4t^2/U$ is dominant in the thermoelectric transport process, leading to small negative S. However, the competition between the second-order interaction t^2 and third-order interaction t^3 suppresses the magnitude of the negative S for 0.2 meV$\lesssim t \lesssim$ 0.26 meV, leading to the charge polarity reversal of the Seebeck coefficient. Accordingly, the sign of S changes from negative to positive at approximately $t \backsimeq 0.26$ meV. When the tunneling strength t increases beyond the value of $t \backsimeq 0.26$ meV, the Seebeck coefficient experiences rapid growth with increasing tunneling strength owing to the chiral interaction formed via the TTQD system. The anomalous behavior of the Seebeck coefficient with the interdot tunneling strength can be understood as follows: a strong tunneling strength links the three spins together to form chiral interactions through three QDs, which breaks the electron–hole symmetry. The electrons contribute to thermoelectric transport, therefore, the electron-like transport is dominant and associated with a negative thermocurrent, leading to a positive S in the thermoelectric transport process through the ring-like TTQD system. Therefore, a large tunneling strength lifts the symmetry of electron–hole transport, leading to a large enhancement of Seebeck coefficient S as a result of the chiral interactions through the TTQD structure. The chiral interaction makes the entire system more stable, assisting thermoelectric transport through the ring-like TTQD system. In addition, the TTQD system makes it easier to adjust the Seebeck coefficient continuously in experiments, which increases the possibility of improving thermoelectric efficiency by adjusting the interdot tunneling strength at the electron–hole symmetry point in the absence of a magnetic field.

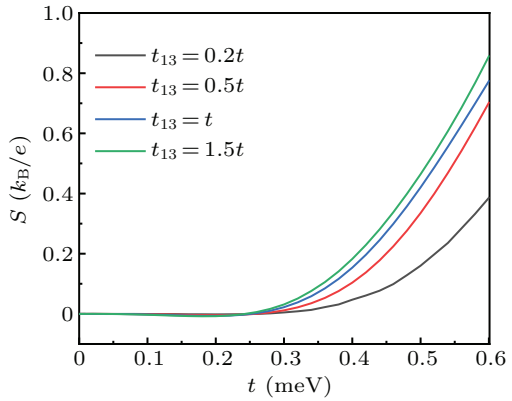


Fig. 2. The Seebeck coefficient S as a function of tunneling strength t ($t_{12} = t_{23} = t$), with different tunneling strengths between QD1 and QD3, $t_{13} = 0.2t$, $0.5t$, t, $1.5t$, in the absence of magnetic field.

Furthermore, for a case of asymmetry structure in the TTQD system, where the interdot tunneling strength t_{13} is different from $t_{12} = t_{23} = t$, the Seebeck coefficient as a function of tunneling strength t is shown in Fig. 2. It is obvious that the Seebeck coefficient increases with tunneling strength t, which is the same as that described in the symmetry structure, $t_{12} = t_{13} = t_{23} = t$. For $t_{13} < t$ (the solid black line and red line), the Seebeck coefficient is smaller than that of the symmetry structure (solid blue line), because the chiral interaction is weaker than that of the symmetry structure. When $t_{13} > t$, the Seebeck coefficient is higher than the symmetry structure (solid green line). Therefore, the tunneling strengths among three QDs are strongly correlated with the magnitude of the Seebeck coefficient, a detailed description is discussed in the following.

As a further investigation, the Seebeck coefficient can be matched properly by combining the tunneling strength with magnetic flux, and this provides an application of the TTQD system using theoretical basis of thermoelectric transport. As shown in Fig. 3(a), the Seebeck coefficient as a function of the tunneling strength, t ($t_{13} = t_{23} = t_{12}$), is calculated at different magnetic flux phases, φ. For φ =0 (solid black line), the sign of S is positive with increasing t, whereas it remains negative at $\varphi = \pi$ (solid purple line), but with the same magnitude as in the case of $\varphi = 0$. Identical behavior appears at $\varphi = 0.25\pi$ (solid red line) and $\varphi = 0.75\pi$ (solid green line). In addition, the magnitude of S is zero when the magnetic flux phase is $\varphi = 0.5\pi$ (solid blue line). Therefore, the numerical computation results demonstrate that the magnitude of the Seebeck coefficient can be changed by tuning the tunneling strength, leading to novel behavior as a result of the chiral interactions

forming through the TTQD system. Meanwhile, the magnetic flux can adjust the sign of the Seebeck coefficient to determine whether electron-like or hole-like transport occurs in the TTQD system.

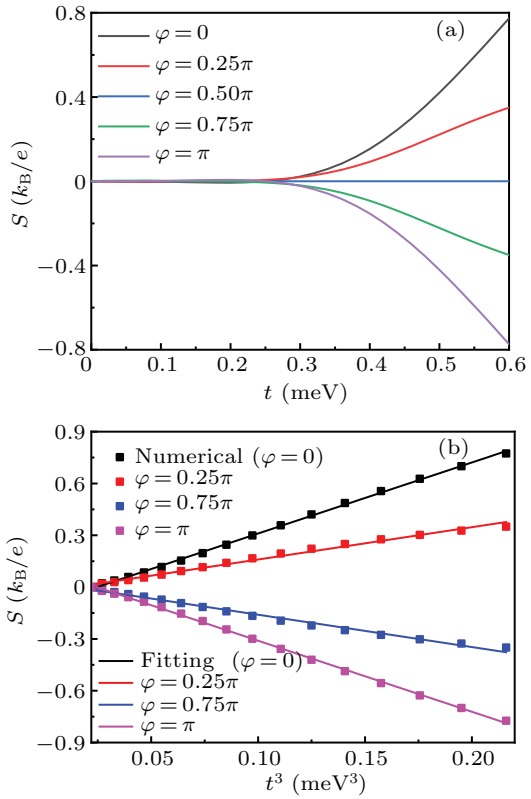


Fig. 3. The Seebeck coefficient S as a function of tunneling strength t ($t_{12} = t_{13} = t_{23}$) at different magnetic flux phases: $\varphi = 0$, $\varphi = 0.25\pi$, $\varphi = 0.5\pi$, $\varphi = 0.75\pi$, and $\varphi = \pi$. We choose large tunneling strength $t \gtrsim 0.26$ meV in (a), and show the linear fitting relation of the Seebeck coefficient dependence on tunneling strength t^3 at different magnetic flux phases in (b), that is, $\varphi = 0$, $\varphi = 0.25\pi$, $\varphi = 0.75\pi$, and $\varphi = \pi$.

To investigate the detailed relationship between the Seebeck coefficient and the tunneling strength, we examine a large tunneling strength ($t \gtrsim 0.26$ meV) in Fig. 3(a), where the Seebeck coefficient shows distinct growth with increasing strength. We also show the linear fitting relation of the Seebeck coefficient dependence on the tunneling strength t^3 at different magnetic flux phases of $\varphi = 0$ (solid black line), $\varphi = 0.25\pi$ (solid red line), $\varphi = 0.75\pi$ (solid blue line), and $\varphi = \pi$ (solid magenta line) in Fig. 3(b). As depicted in Fig. 3(b), the magnitude of the Seebeck coefficient is perfectly linear with respect to t^3. Consequently, the Seebeck coefficient is closely related to the chiral interaction induced by the three spins through the TTQD structure, making the system more stable and assisting the thermoelectric transport.

3.2. Magnetic field dependence of thermoelectric transport properties

As is well known, the quantum interference effect plays a significant role in thermoelectric transport. For the TTQD system, it is very convenient to obtain the influence of the interference on the thermoelectric quantities by tuning the magnetic flux, threading into a ring-like structure. These thermoelectric quantities are periodic functions in the magnetic flux phase φ, with a period of 2π or π. The magnetic flux phase resulting from the phase factor $t\,e^{i\phi/3}$, where ϕ is the magnetic flux, threads the TTQD system.

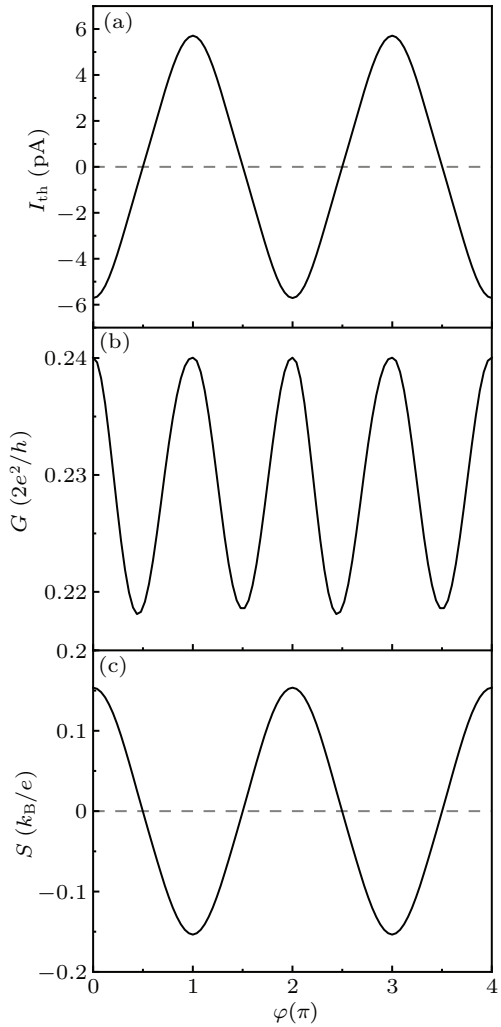


Fig. 4. (a) Thermocurrent I_{th}, (b) conductance G, and (c) Seebeck coefficient S, versus magnetic flux phase φ, under a perpendicular magnetic field at the system temperature $k_BT = 0.2$ meV, with a large tunneling strength $t_{12} = t_{23} = t_{13} = t = 0.4$ meV.

At the electron–hole symmetry point ($\varepsilon = -U/2$), the number of electrons tunneling through the QDs system is equal to the number of tunneling holes. Therefore, the total thermocurrent through QD and double-QD systems is zero.[21] However, because of the presence of tunneling term in the TTQD system, the numbers of electrons and holes are not naturally identical under the electron–hole transition of the Hamiltonian of an isolated TTQD system at the point $\varepsilon = -U/2 = -1$ meV. The numbers of electrons and holes will recover being identical when a perpendicular magnetic field is applied to the TTQD system.[45] Existing studies show that the sign of the thermocurrent reflects the dominance of the electron (−) or hole (+) transport in the thermoelectric transport process through a QD system.[11,21] Therefore, the thermocur-

rent can be seen as an observation to detect either hole-like or electron-like transport through the QDs system.

We choose a large tunneling strength of $t = 0.4$ meV where the chiral interaction term χ will react and present a diagram of the thermocurrent $I_{\rm th}$ as a function of magnetic flux phase φ in Fig. 4(a). It is seen that $I_{\rm th}$ is a periodic function in φ with a period of 2π. In detail, the sign of the thermocurrent is negative at the point of $\varphi = 0$, which indicates electron-like transport through the system without a magnetic field. The thermocurrent varies from negative to positive when changing the magnitude of the magnetic flux with a period of 2π, and $I_{\rm th}$ experiences a zero point at $\varphi = \pi/2 + k\pi$ $(k = 0, 1, 2\ldots)$. Therefore, the electron–hole will become symmetric at a specific magnetic flux of $\varphi = \pi/2 + k\pi$ $(k = 0, 1, 2\ldots)$ in the TTQD system. In addition, as shown in Fig. 4(b), the magnitude of the conductance G manifests as a periodic function in φ with a period of π. In detail, the G reaches minima at $\varphi = \pi/2 + k\pi$ $(k = 0, 1, 2\ldots)$ and maxima at $k\pi$ $(k = 0, 1, 2\ldots)$. The Seebeck coefficient is calculated via the thermocurrent divided by the conductance. Therefore, the Seebeck coefficient has the same period as that of the thermocurrent. The amplitude of the Seebeck coefficient as a function of the magnetic flux (Fig. 4(c)) indicates that the charge polarity reversal of the Seebeck coefficient from positive to negative, and vice versa, is induced by the regulation of the magnetic flux.

3.3. On-site energy dependence of the thermoelectric transport properties and violation of the Mott relation

As mentioned above, we have discussed the thermoelectric transport properties via the TTQD system under the condition of electron–hole symmetry. In general, the QDs system can be tuned from the Kondo to the mixed-valence or empty-orbital regimes via the gate voltage,[20] leading to novel thermoelectric transport properties. Previous studies of the thermoelectric properties by altering the gate voltage mainly involving two-level QD[12] and single-level QD,[21] indicating that the Kondo resonance assists thermoelectric transport through strongly correlated QD at low temperatures. Experimentally, the thermopower shows a clear deviation from the semiclassical Mott relation in the vicinity of the spin Kondo correlation regimes.[11] In this work, we also observe the phenomenon of the violation of semiclassical Mott relation, because the Kondo effect induced on QD2 at low temperature, as well as the spin chiral interactions formed in the TTQDs system, assists thermoelectric transport.

We calculate the Seebeck coefficient as a function of the on-site energies under a low temperature of $k_{\rm B}T = 0.05$ meV, as shown in Fig. 5, and we choose a large interdot tunneling strength $t = 0.4$ meV, where the chiral interactions act through the TTQD system. As shown in Fig. 5, the numerical computation results for the Seebeck coefficient show a nonmonotonic behavior with increasing on-site energies ε in the range of -2 meV$\lesssim \varepsilon \lesssim 0.5$ meV, remaining in the Kondo and mixed-valence regimes. In the Kondo regime, the occupancy for QD2 is nearly 1 and a localized spin formed on the dot at $k_{\rm B}T = 0.05$ meV, where the on-site energy is approximately -1.5 meV$\lesssim \varepsilon \lesssim -0.5$ meV. Physical properties are characterized by spin fluctuations in this regime. Therefore, there are two sign changes of the Seebeck coefficient arising at $\varepsilon \simeq -1.5$ meV and $\varepsilon \simeq -0.5$ meV. The Kondo singlet state forming between the QD2 and conduction electrons will assist the transport process, contributing to a positive Seebeck coefficient. In the mixed regime, the charges fluctuates between 0 and 1 resulting in an average occupation number of 0.5, so the physical mechanism is governed by the charges together with the spin fluctuations, contributing to complex behavior of thermoelectric transport. The magnitude of S oscillates with the increasing on-site energy, arising at -2 meV$\lesssim \varepsilon \lesssim -1.5$ meV and -0.5 meV$\lesssim \varepsilon \lesssim 0.5$ meV, because of the interference effects of the charges together with the spin fluctuations at low temperature.

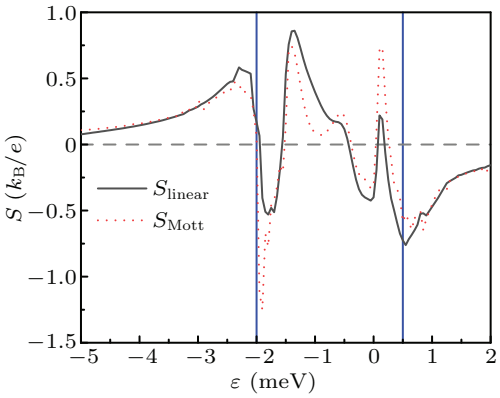


Fig. 5. The Seebeck coefficient calculated by Eq. (1) (dashed red line) in comparison with Eq. (6) (solid black line) at the temperature, $k_{\rm B}T = 0.05$ meV, in the absence of magnetic field. The blue solid lines divide the space into three physical regions, where -2 meV$\lesssim \varepsilon \lesssim -1.5$ meV and -0.5 meV$\lesssim \varepsilon \lesssim 0.5m$ eV is the mixed-valence regime, -1.5 meV$\lesssim \varepsilon \lesssim -0.5$ meV is the Kondo regime, 0.5 meV$\lesssim \varepsilon \lesssim 2$ meV is the empty orbital regime. The electron–hole symmetry point is $\varepsilon_{\rm sys} = -U/2 = -1$ meV and the interdot tunneling strength set as $t_{12} = t_{23} = t_{13} = 0.4$ meV.

We compare the Seebeck coefficient calculated using Eq. (1) (dashed red lines) with that calculated using Eq. (6) (solid black lines) in the linear regime, as depicted in Fig. 5 ($k_{\rm B}T = 0.05$ meV). The numerical computation results show a clear deviation from the semiclassical Mott relation in the range of Kondo and mixed regimes (-2 meV$\lesssim \varepsilon \lesssim 0.5$ meV). A comparison between $S_{\rm linear}$ and the semiclassical expected $S_{\rm Mott}$ shows the additional contributions of the thermopower in the Kondo and mixed-valence regimes, where spin correlations induced by the Kondo effect is a prime candidate for explaining the occurrence of these extra contributions. In addition, the chiral interaction also acts through the TTQD system. With increasing the interdot tunneling t, the three quan-

tum dots are tied together to make the system more stable, assisting the thermal transport of electrons. Therefore, $S_{\rm linear}$ and $S_{\rm Mott}$ show a complex nonmonotonic behavior with an increasing magnitude because of the Kondo effect together with the chiral interaction-assisted thermoelectric transport.

4. Summary

We have theoretically investigated the thermoelectric transport properties in a ring-like TTQD system with one dot coupled to two leads. We examine the thermoelectric effect dependence on the tunneling strength, magnetic flux, and on-site energy and find that a large enhancement of the Seebeck coefficient arises through the TTQD structure, which results from the spin chiral interaction with increasing the interdot tunneling t. At the electron–hole symmetry point, with the increasing interdot tunneling strength t, the numerical results indicate that the Seebeck coefficient is linear with respect to the tunneling strength t^3 for different values of the magnetic flux. Therefore, the magnitude of the Seebeck coefficient could be adjusted by the interdot tunneling, and the charge polarity reversal of the Seebeck coefficient is linked to the magnetic flux. Under a perpendicular magnetic field, the quantum interference effect plays a significant role in the thermoelectric transport, where the Seebeck coefficient, thermocurrent, and conductance are periodic functions of the magnetic flux phase through the TTQD system. Moreover, at low temperature, the Seebeck coefficient dependence on the on-site energy indicates that the semiclassical Mott relation between the thermopower and conductance is failed to describe the asymmetry of the electron–hole transport in the Kondo and mixed-valence regimes, since the many-body effects of the Kondo correlation induced resonance act as well as the spin chiral interaction work through the TTQD system.

Acknowledgements

Computational resources were provided by the Physical Laboratory of High Performance Computing at Renmin University of China.

Project supported by the National Natural Science Foundation of China (Grant Nos. 11774418, 11374363, and 21373191).

References

[1] Franz R and Wiedemann D 1853 *Ann. Phys.* **165** 497
[2] Ashcroft N W and Mermin N D 1976 *Solid State Physics* (Stanford: Cengage Learning)
[3] Turek M and Matveev K A 2002 *Phys. Rev. B* **65** 115332
[4] Kubala B, König J and Pekola J 2008 *Phys. Rev. Lett.* **100** 066801
[5] Vavilov M G and Stone A D 2005 *Phys. Rev. B* **72** 205107
[6] Murphy P, Mukerjee S and Moore J 2008 *Phys. Rev. B* **78** 161406(R)
[7] Wierzbicki M and Świrkowicz R 2010 *Phys. Rev. B* **82** 165334
[8] Liu J, Sun Q F and Xie X C 2010 *Phys. Rev. B* **81** 245323
[9] Nguyen T K T, Kiselev M N and Kravtsov V E 2010 *Phys. Rev. B* **82** 113306
[10] Gong W J, Wang H M, Han Y and Zhang S J 2010 *Curr. Appl. Phys.* **82** 113306
[11] Scheibner R, Buhmann H, Reuter D, Kiselev M N and Molenkamp L W 2005 *Phys. Rev. Lett.* **95** 176602
[12] Ye L Z, Hou D, Wang R L, Cao D W, Zheng X and Yan Y J 2014 *Phys. Rev. B* **90** 165116
[13] Wang Q, Xie H Q, Nie Y H and Ren W 2013 *Phys. Rev. B* **87** 075102
[14] Blanter Y M, Bruder C, Fazio R and Schoeller H 1997 *Phys. Rev. B* **55** 4069
[15] Kim T S and Hershfield S 2002 *Phys. Rev. Lett.* **88** 136601
[16] Staring A A M, Molenkamp L W, Alphenaar B W, Van Houten H, Buyk O J A, Mabesoone M A A, Beenakker C W J and Foxon C T 1993*Europhys. Lett.* **22** 57
[17] Scheibner R, Novik E G, Borzenko T, König M, Reuter D, Wieck A D, Buhmann H and Molenkamp L W 2007 *Phys. Rev. B* **75** 041301(R)
[18] Ziman J M 1960 *Electrons and Phonons* (New York: Oxford University Press)
[19] Cutler M and Mott N F 1969 *Phys. Rev.* **181** 1336
[20] Costi T A and Zlatić V 2010 *Phys. Rev. B* **81** 235127
[21] Cheng Y X, Li Z H, Wei J H, Luo H G, Lin H Q and Yan Y J 2020 *Sci. China Phys. Mech. Astron.* **63** 297811
[22] Gaudreau L, Studenikin S A, Sachrajda A S, Zawadzki P, Kam A, Lapointe J, Korkusinski M and Hawrylak P 2006 *Phys. Rev. Lett.* **97** 036807
[23] Mitchell A K, Jarrold T F, Galpin M R and Logan D E 2013 *J. Phys. Chem. B* **117** 12777
[24] Hsieh C Y, Shim Y P, Korkusinski M and Hawrylak P 2012 *Rep. Prog. Phys.* **75** 114501
[25] Cheng Y X, Wang Y D, Wei J H, Zhu Z G and Yan Y J 2017 *Phys. Rev. B* **95** 155417
[26] Weymann I, BuŁka B R and Barnaś J 2011 *Phys. Rev. B* **83** 195302
[27] Niklas M, Trottmann A, Donarini A and Grifoni M 2017 *Phys. Rev. B* **95** 115133
[28] Chen C C, Kuo D M T and Chang Y C 2015 *Phys. Chem. Chem. Phys.* **17** 19386
[29] Sun L L, Chi F, Fu Z G, Yu S C, Liu L M and Chen H W 2019 *J. Low. Temp. Phys.* **194** 235
[30] Taguchi Y, Oohara Y, Yoshizawa H, Nagaosa N and Tokura Y 2001 *Science* **291** 2573
[31] Scarola V W, Park K and Das Sarma S 2004 *Phys. Rev. Lett.* **93** 120503
[32] Hsieh C Y, Rene A and Hawrylak P 2012 *Phys. Rev. B* **86** 115312
[33] Wang Y D, Zhu Z G, Wei J H and Yan Y J 2020 *Europhy. Lett.* **130** 17003
[34] Scarola V W and Das Sarma S 2005 *Phys. Rev. A* **71** 032340
[35] Wen X G, Wilczek F and Zee A 1989 *Phys. Rev. B* **39** 11413
[36] Li Z H, Tong N H, Zheng X, Hou D, Wei J H, Hu J and Yan Y J 2012 *Phys. Rev. Lett.* **109** 266403
[37] Ye L Z, Wang X L, Hou D, Xu R X, Zheng X and Yan Y J 2016 *WIREs Comput. Mol. Sci.* **6** 608
[38] Feynman R P and Vernon F L 2000 *Ann. Phys.* **281** 547
[39] Jin J S, Zheng X and Yan Y J 2008 *J. Chem. Phys.* **128** 234703
[40] Yan Y J 2014 *J. Chem. Phys.* **140** 054105
[41] Yan Y J, Jin J S, Xu R X and Zheng X 2016 *Front. Phys.* **11** 110306
[42] Wang Y D, Ni J H and Wei J H 2017 *Phys. Rev. B* **96** 245426
[43] Cheng Y X, Wang Y D, Wei J H, Zhu Z G and Yan Y J 2017 *Phys. Rev. B* **95** 155417
[44] Li Z H, Cheng Y X, Wei J H, Zheng X and Yan Y J 2018 *Phys. Rev. B* **98** 115133
[45] Liu Y M, Wang Y D and Wei J H 2022 *Chin. Phys. B* **31** 057201